

## Comparison of the energy resolution of the standard and totally active scintillator detectors

Peter Litchfield and Leon Mualem

A feature of the totally active (TA) Nova detector design which could offer an important advantage over the standard (SD) design is the improved energy resolution provided by the much larger fraction of active detector. In this note a comparison is made of the resolution in the two detectors.

The SD detector simulation was described in Nova notes 24 and 42. The TA detector simulation was generated by Leon Mualem and used for the note “Update on Totally Active Scintillator Detector (TASD)” by Stan Wojcicki. The light collection simulation was the same for each detector with the same (35 pe) mean light output at the far end of the 15m and 17m strips for a normal minimum ionizing particle.

The run conditions were 810 km from Fermilab, 12km off-axis,  $\Delta m^2=0.0025 \text{ eV}^2$   $\sin^2 2\theta_{13}=0.10$ . Only  $\nu_e$  CC events oscillated from  $\nu_\mu$  are considered in this note.

The same reconstruction codes were used for both detectors. The same event selection chain was used as in Nova-NOTE-SIM-42, except that the cut on number of hits/plane in the Hough track was moved before the cut on the fraction hits in the Hough track. The hits/plane cut essentially defines an electron track. This selection chain more closely resembles that used by Stan. The same selections were used for each detector with the cuts optimized in each case to produce the best FOM.

The resolution was obtained under five analysis conditions;

1. All generated events
2. Events that passed the reconstruction and containment cuts
3. Events that had a reconstructed electron track and passed the length and total pulse height cuts (as in SIM-42)
4. Events that passed the remaining cuts but before the likelihood analysis
5. Selected events.

The  $\nu$  energy resolution is characterized by the variable (called *DELE* after Stan)

$$DELE = \frac{(\text{Measured energy} - \text{Truth energy})}{\sqrt{\text{Truth energy}}}$$

The measured energy is taken as the summed pulse height of the event, normalized to give a zero mean for *DELE* summed over all selected events. The truth energy is taken from the MC generated parameters.

It is well known that the summed pulse height is dependent on the relative fraction of hadronic and electromagnetic showers in the final state and thus on the fraction of the total pulse height in the electron track (PHE). The left plot in Figure 1 shows *DELE* plotted against PHE after the cuts defining an electron track (stage 3), for the TA events. A clear dependence on PHE can be seen. A linear correction for this

effect has been applied by adding  $0.3 \cdot (1.0 - \text{PHE})$  to DELE. The right hand plot shows the same data after correction. Figure 2 shows the same plots for the SD. The same correction has been applied. More sophisticated corrections could be envisaged, particularly if a fuller reconstruction of the events was made that identified more individual tracks. However the resolutions found here are comparable with those in Stan's note which did a more complete reconstruction, indicating that maybe there is not too much to gain.

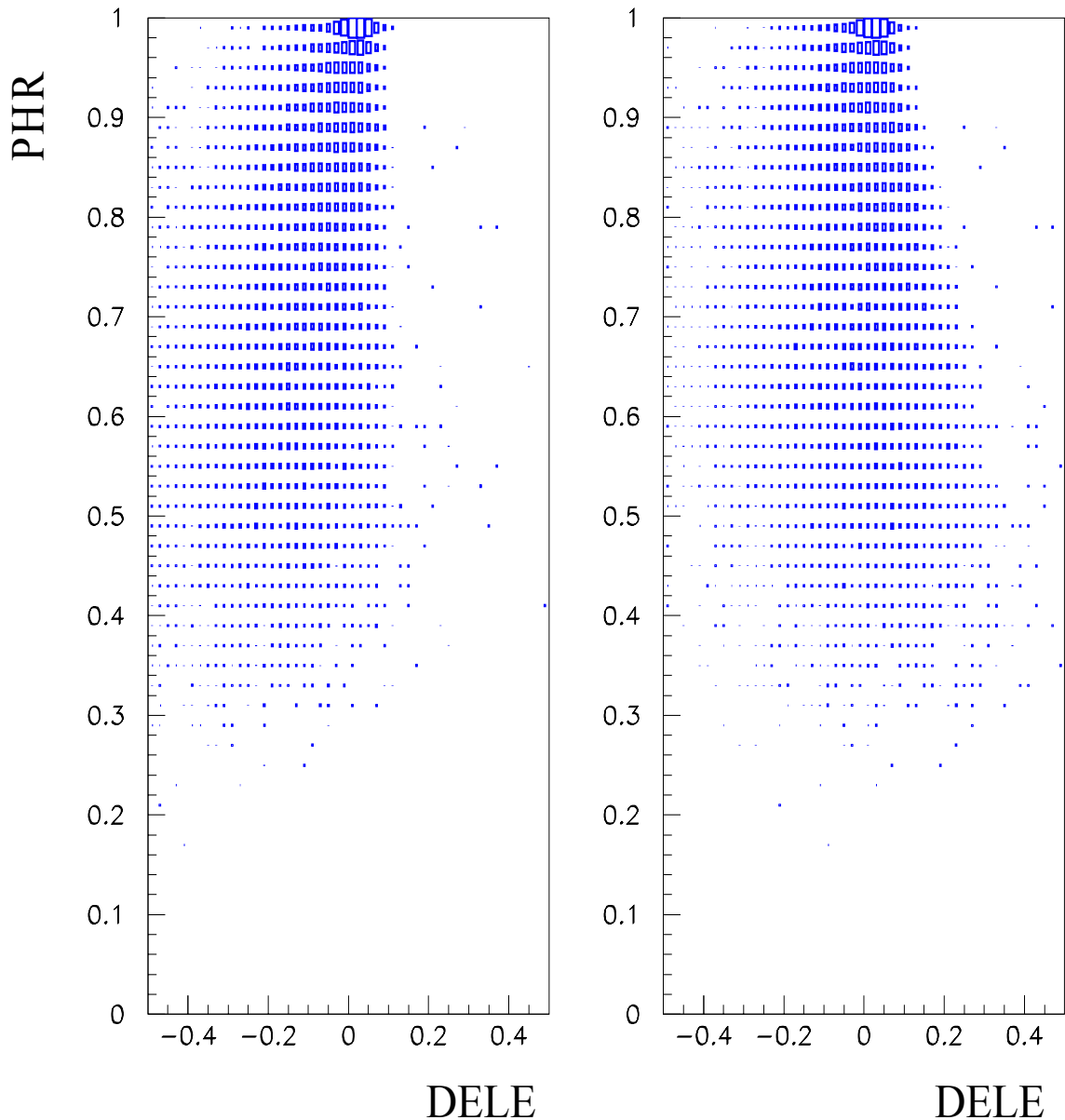


Figure 1: Dele plotted against the fraction of the total pulse height in the electron track (proportional to  $1-y$ ) for the totally active detector. Uncorrected in the left plot and corrected in the right plot

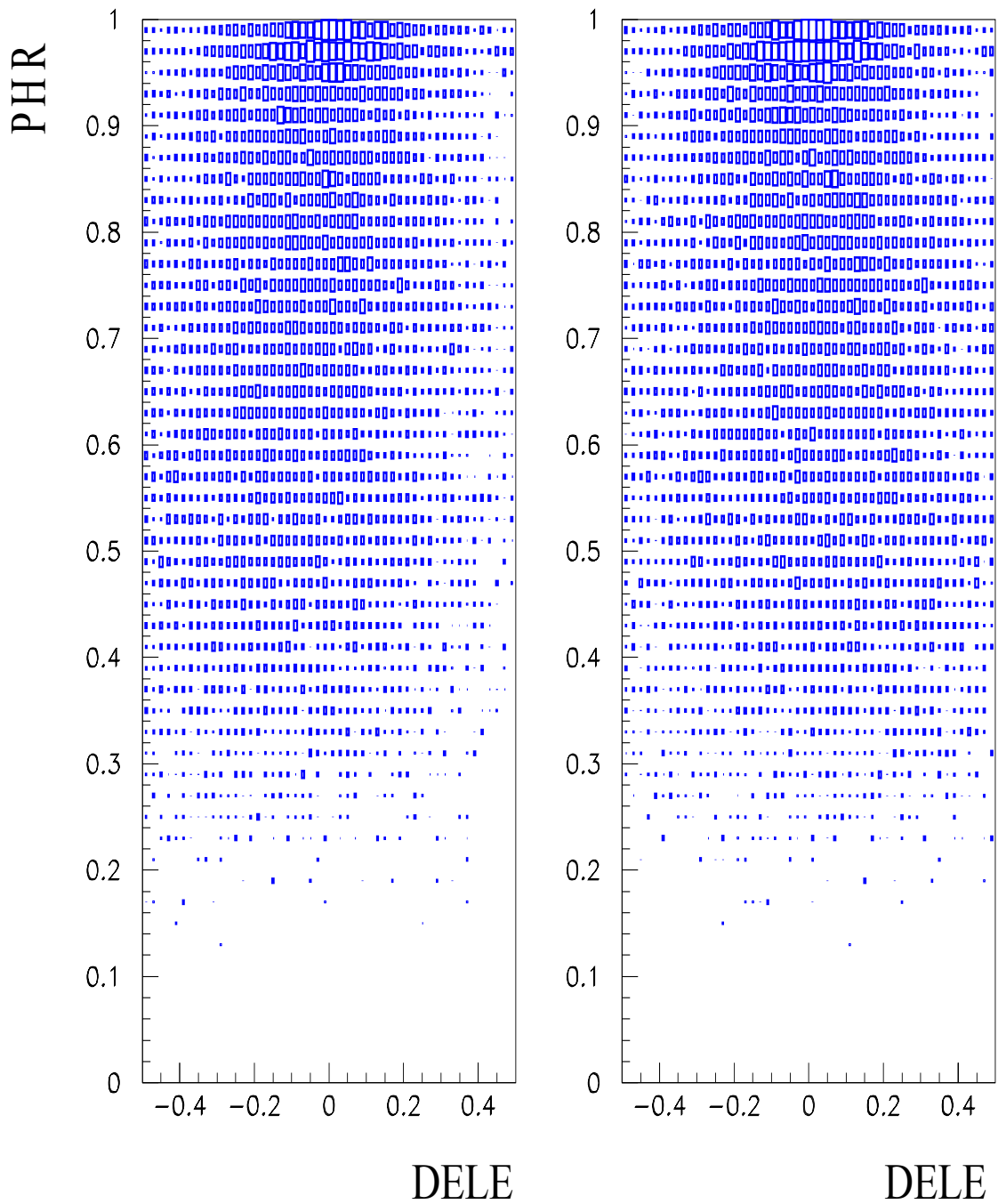


Figure2: Dele plotted against the fraction of the total pulse height in the electron track (proportional to  $1-y$ ) for the standard detector. Uncorrected in the left plot and corrected in the right plot

Figure 3 shows histograms of  $DELE$  at the five points in the analysis for the TA detector. The events are weighted by the beam spectrum and the  $\nu_{\mu} \rightarrow \nu_e$  oscillation probability. Figure 4 shows the same quantities for the SD detector.

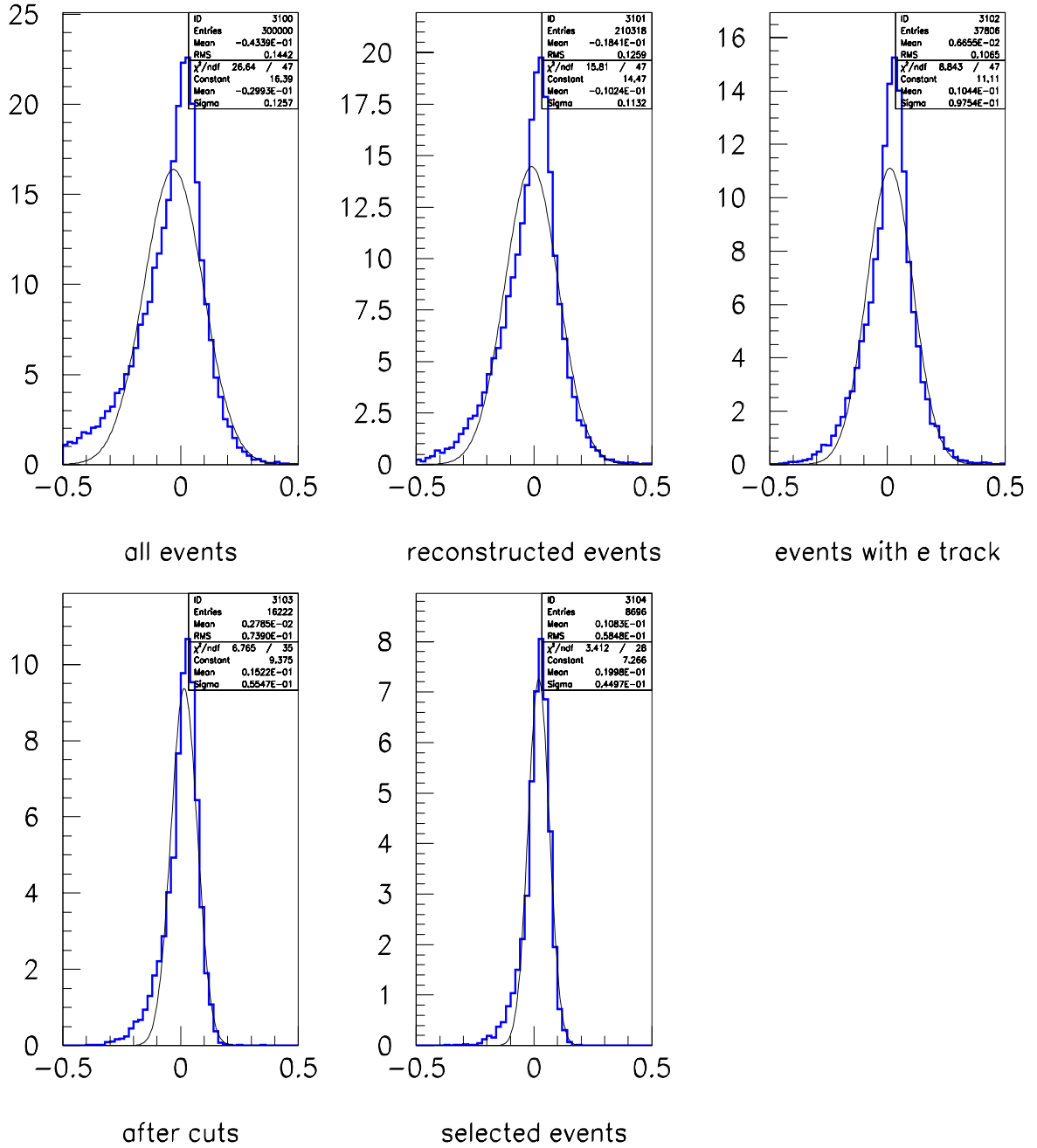


Figure 3: Histograms of  $DELE$  at various points in the analysis chain for the totally active detector. From top left to bottom right; all events, events after reconstruction and the containment cut, events with an identified electron, events after the cuts but before the likelihood analysis, final selected electron sample.

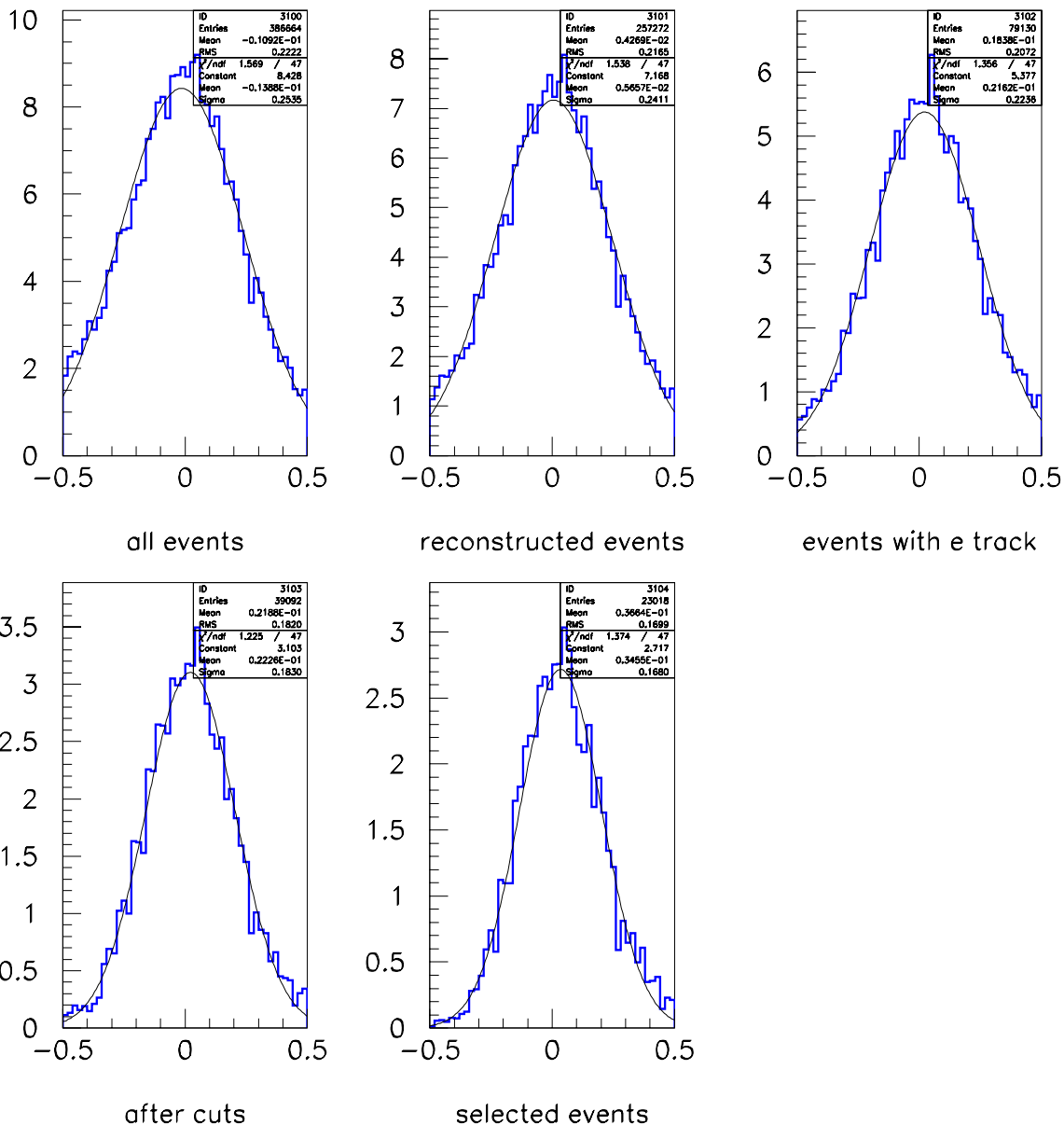


Figure 4: Histograms of DELE at various points in the analysis chain for the standard detector. From top left to bottom right; all events, events after reconstruction and the containment cut, events with an identified electron, events after the cuts but before the likelihood analysis, final selected electron sample.

Gaussian functions have been fitted to the distributions in Figures 3 and 4 and the width parameters are given in table 1 for all events with an identified electron and the final selected samples.

	Electron events	Final sample
SD	0.224	0.168
TA	0.098	0.045

**Table 1:** Gaussian width of DELE for the SD and TA detectors, for electron events and the finally selected sample.

The width for the electron event sample in the TA detector is consistent with that found by Stan (0.097) for his selected electron sample, though his correction and electron selection was somewhat more sophisticated. The standard detector electron event width is compatible with the RPC width of 0.23 quoted by John Cooper in his PAC talk, though the analysis procedures of the RPC analysis are different from those in this note. The summed pulse height measurement would be expected to give a better resolution than a summed hit measurement.

It has been noted that with good enough resolution the data could be divided into energy bins across the oscillation peak in order to see the variation of oscillation probability with energy predicted by matter effects, and thus obtain a better measurement of the sign of  $\Delta m^2$ . Figure 5 shows the truth energy distributions for three equally spaced regions of total pulse height (measured energy) for the finally selected sample in the totally active detector and Figure 6 the same for the standard detector. It can be seen that the totally active detector offers a significantly better energy binning than the standard detector.

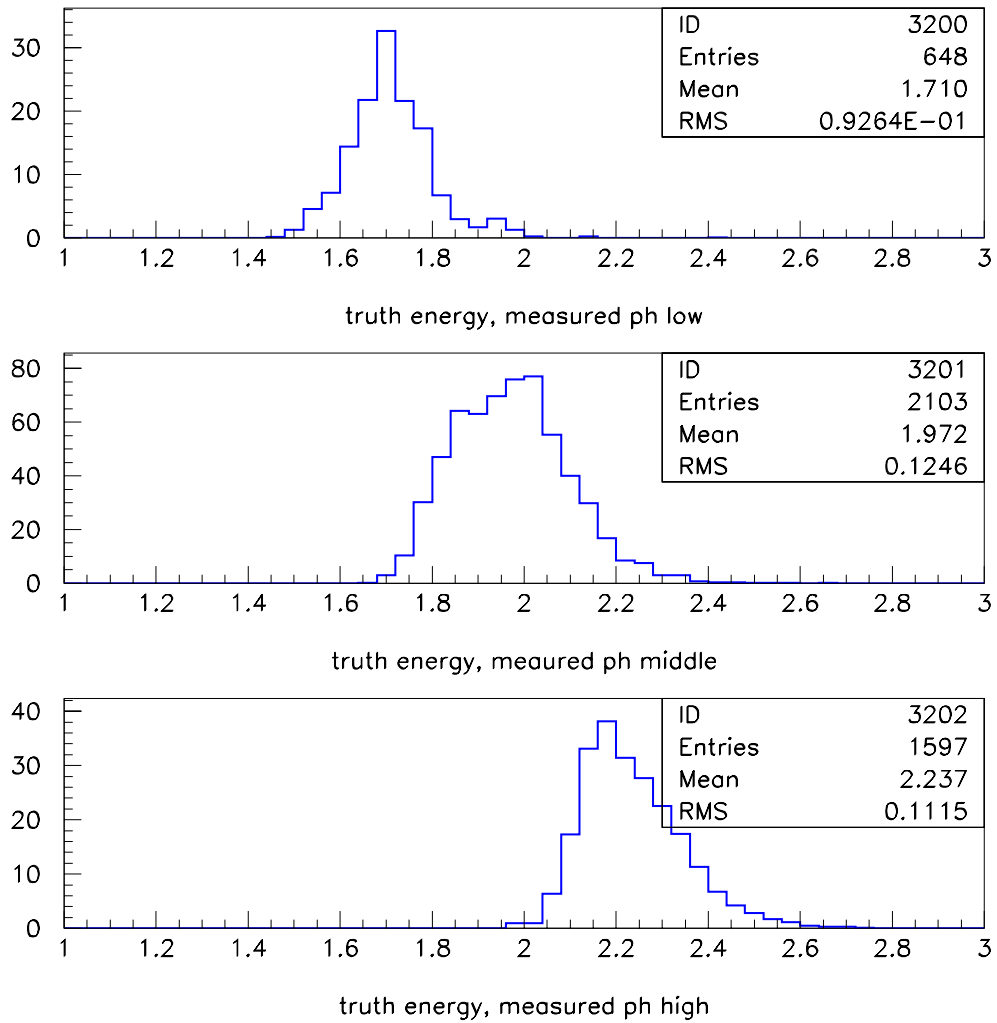


Figure 5: Truth energy in GeV for three regions of measured total pulse height for the totally active detector

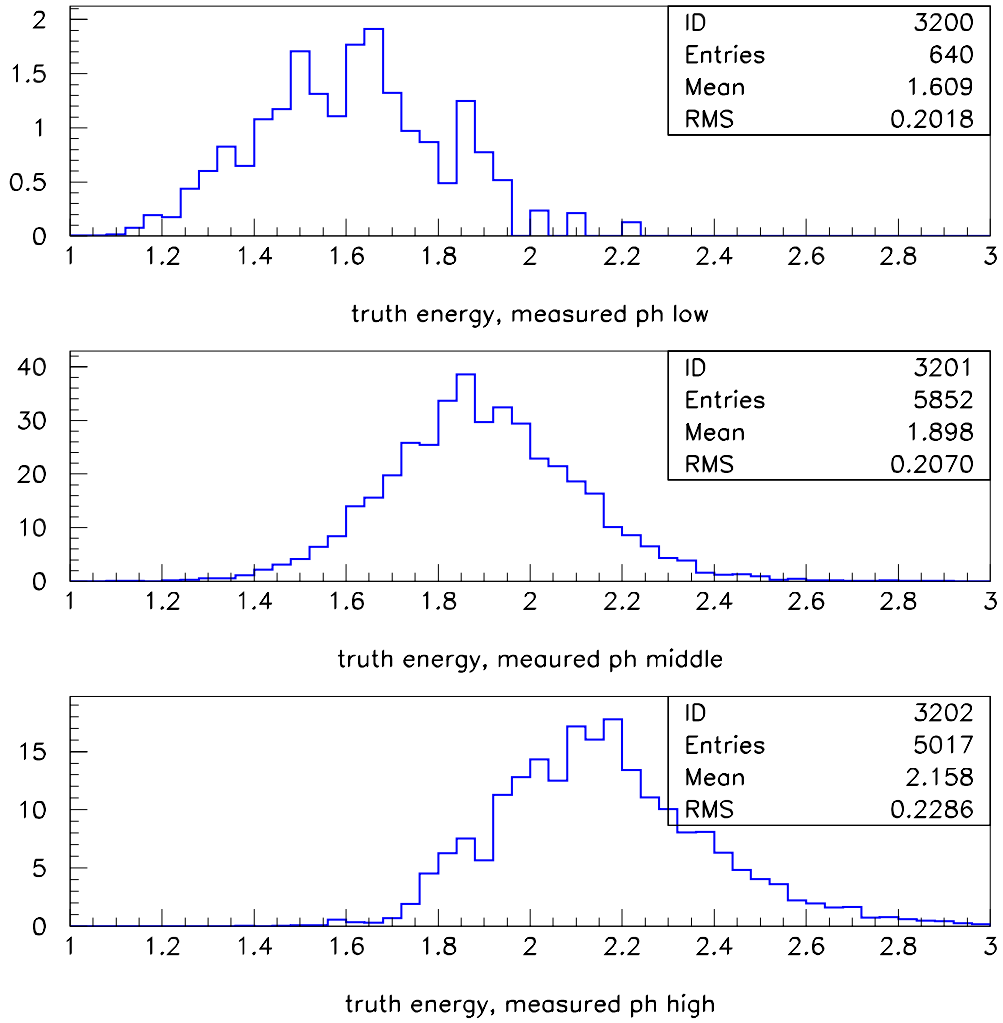


Figure 6: Truth energy in GeV for three regions of measured total pulse height for the standard detector